CHAPTER 3

Chapter 3

Synthesis and Characterization of Peroxoniobium(V) Complexes Anchored to Water Soluble Polymers

Contents

This work deals with the synthesis of two novel macrocomplexes, water soluble polymer-anchored pNb complexes, $[Nb_2(O_2)_6(carboxylate)_2]$-PA [PA = poly(sodium acrylate)] **(PANb) (3.1)** and $[Nb(O_2)_3(sulfonate)_2]$-PSS [PSS = poly(sodium styrene sulfonate)] **(PSSNb) (3.2)**. The developed compounds were characterized by elemental analysis (CHN, ICP and energy-dispersive X-ray spectroscopy), spectral studies (IR, ^{13}C and ^{93}Nb NMR studies), thermogravimetric analysis (TGA) as well as SEM studies. The structures of **PANb** and **PSSNb** have also been studied by density functional theory (DFT) method.

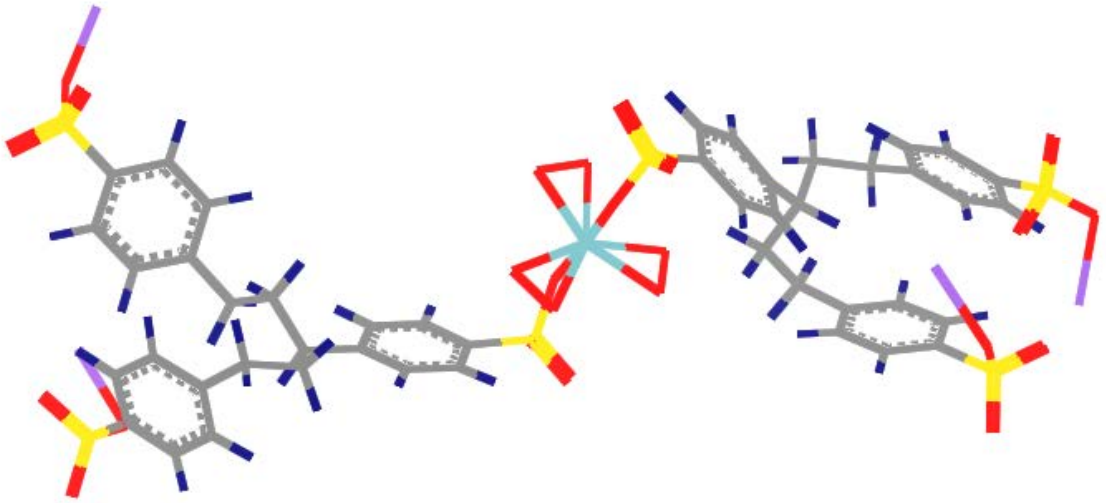

3.1 Introduction

Development of macromolecular metal complexes using water soluble polymers (WSPs), as emphasized in the literature and highlighted in the Chapter 1, is emerging as a promising trend in the field of metal containing polymers which is interesting from both chemical as well as biological perspectives [1-3]. Our interest in anchoring pNb species to WSPs has been stimulated by the prospect of generating potential water tolerant oxidation catalysts applicable in aqueous medium, as well as by the possibility of obtaining pNb containing macrocomplexes with bio-relevant features. In contrast to the availability of multitude of reports dealing with heteroleptic pNb derivatives with variety of ancillary ligands [4-11], no information appears to exist on peroxoniobates where a functionalized macromolecule provides the co-ligand environment.

One of the very important characteristics of a soluble polymer supported reagent is the facility of product synthesis and characterization provided by such a support due to the advantages of homogeneity offered by it [12,13]. Moreover, polymers are often free from inconvenient properties of monomeric species, such as lability, volatility, toxicity and odour [14]. Therefore, the importance of linking drug molecules, including low molecular weight metal complexes, to soluble macromolecular carriers can be readily appreciated since such systems are likely to overcome the limitations such as toxic side effects by improving the body distribution of drugs and prolonging their activity [15-18].

It is pertinent to mention that other workers of our research group successfully synthesized a series of stable and well-defined macrocomplexes with peroxo species of vanadium (pV) [19-21], molybdenum (pMo) [20-22] and tungsten (pW) species [23] anchored to the WSPs matrices. To the best of our knowledge, these complexes have been the first reported examples of peroxometallates attached to water soluble polymers. Several of these macro complexes exhibited unique biochemical as well as oxidant properties [21] including antibacterial, enzyme inhibitory and vasomodulatory activities [24]. Recently, it has been demonstrated that peroxovanadate immobilized on poly(acrylic acid) becomes a highly potent inhibitor of growth of lung carcinoma cells (A549) [25]. These interesting observations reveal that a lot remains yet to be explored regarding other possible chemical and biochemical aspects of these compounds. In fact, anchoring of peroxometallates to WSP has recently been recognized as a promising new

field [26]. Thus, there is an obvious need to broaden the panel of this class of new materials preferably by establishing easy synthetic procedures.

A polymeric support usually enhances stability of the anchored complex species and proper choice of the functional group is an important prerequisite in order to establish a robust polymer-metal linkage [27]. For practical application of WSPs, such systems are required to possess certain desirable features such as: (i) chemical stability and high hydrophilicity, (ii) an easy and cost effective route of synthesis, (iii) an adequate molecular weight distribution and (iv) high affinity to bind metal ions [27].

For the present study, we selected WSPs with two different types of pendant ligand groups *viz.*, poly(acrylic acid) (PAA) and poly(sodium 4-styrene sulfonate) (PSS) since, in addition to fulfilling all of the above criteria, these polymers are biocompatible, and there has been considerable contemporary interest in development of pharmaceutical formulations based on acrylate and sulfonate containing polymers and their derivatives [28-36]. Interestingly, poly(sodium 4-styrene sulfonate), a cation exchanger resin, has been reported to be effective in treatment of lithium toxicity [37]. On the other hand, poly(sodium acrylate) is one of the preferred water-soluble anionic polyelectrolytes used as dispersing agent, superabsorbent polymer and ion-exchange resin [38]. It has been reported that PAA and its derivatives are broadly used as polymeric carriers for proteins, enzymes, drugs and other biologically active molecules [39,40]. In addition, because of low toxicity, they are used as a food additive [38]. Most importantly, PAA chain can provide carboxylate groups which are among the most suitable ligands for niobium(V) ion co-ordination [4,8-11].

This chapter describes the synthesis and characterization of a pair of new water soluble polymer anchored pNb macrocomplexes of the type, $[Nb_2(O_2)_6(carboxylate)_2]$-PA [PA = poly(sodium acrylate)] **(PANb) (3.1)** and $[Nb(O_2)_3(sulfonate)_2]$-PSS [PSS = poly(sodium styrene sulfonate)] **(PSSNb) (3.2)**.

3.2 Experimental section

3.2.1 $Na_3[Nb(O_2)_4]\cdot 13H_2O$ (NaNb) synthesis [41]

The precursor complex, $Na_3[Nb(O_2)_4]\cdot 13H_2O$, was prepared by fusing 1 g of Nb_2O_5 with 1.85 g of NaOH in a nickel crucible at 700 °C, as has been reported

previously [41]. The solid product was cooled and subsequently dissolved in 100 mL of 1 M aqueous H_2O_2. Unreacted Nb_2O_5 was filtered off and the filtrate was allowed to stand at 5 °C for 24 h to obtain the crystals of $Na_3[Nb(O_2)_4]\cdot 13H_2O$.

3.2.2 Synthesis of $[Nb_2(O_2)_6(carboxylate)_2]$-PA (PANb) (3.1)

To a solution of the precursor complex sodium tetraperoxoniobate, $Na_3[Nb(O_2)_4]\cdot 13H_2O$ (0.68 g, 1.3 mmol) in 30% H_2O_2 (5 mL, 44 mmol), the WSP poly(sodium acrylate) (**PA**) (0.50 g) was added in portions with constant stirring, maintaining the temperature below 4 °C. The mixture was kept under continuous stirring for *ca*. 1 h in an ice-bath until all solids dissolved. At this stage, the pH of the reaction medium was observed to be *ca.* 7.0. The pH of the solution was subsequently lowered to *ca.* 5.0 by dropwise addition of dilute HNO_3 (4 M) to it with constant stirring. After being allowed to stand for about 3 h in an ice-bath, the solution was treated with pre-cooled acetone to induce precipitation, under vigorous stirring. A white pasty mass separated out from the reaction mixture. The supernatant liquid was decanted off and the residue obtained was treated repeatedly with acetone under scratching. The microcrystalline product was separated by centrifugation, washed with cold acetone and dried *in vacuo* over concentrated sulfuric acid.

3.2.3 Synthesis of $[Nb(O_2)_3(sulfonate)_2]$-PSS (PSSNb) (3.2)

Sodium tetraperoxoniobate, $Na_3[Nb(O_2)_4]\cdot 13H_2O$ (0.68 g, 1.3 mmol) was dissolved in 5 mL (44 mmol) of 30% H_2O_2 and then HNO_3 solution (*ca.* 4 M) was added to the above solution dropwise with constant stirring to maintain the pH of the reaction medium to 5.0. Keeping the temperature of the reaction mixture below 4 °C in an ice bath, 1 mL of 30% poly(sodium 4-styrene sulfonate) (**PSS**) was added to it. The pH of the mixture was recorded to be *ca.* 5.0. After 3h of contact time, solvent induced precipitation was carried out by adding pre-cooled acetone under vigorous stirring. After being allowed to stand for 30 min, the supernatant liquid was decanted off and the residue was repeatedly washed with pre-cooled acetone under scratching. The microcrystalline product was separated by centrifugation and dried *in vacuo* over concentrated sulfuric acid.

3.2.4 Elemental analysis and physical measurements

The niobium, peroxide, carbon, hydrogen, sulfur and sodium content in the synthesized compounds were quantitatively determined by procedures described in Chapter 2. The analytical data of the compounds are summarized in **Table 3.1.** The methods employed for scanning electron micrographs (SEM) and EDX analysis, TG analysis, as well as spectroscopic measurements have been outlined in Chapter 2. Listed in **Table 3.2** are the structurally significant IR and Raman bands along with their assignments. ^{13}C and ^{93}Nb NMR spectra of the complexes are presented in **Fig. 3.9 - Fig. 3.11**.

3.2.5 Computational details

Theoretical investigation has been carried out using density functional theory (DFT) as implemented in $DMol^3$ program package [42,43]. As polymeric structures bind through van der Waals interactions, it is necessary to include these interactions while performing theoretical calculations of the minimum energy structure on the potential energy surface (PES). We have therefore used dispersion corrected density functional theory (DFT-D). Local density models, such as the VWN (Vosko, Wilk and Nusair) [44] functional are among the simplest and computationally efficient. The geometry of the complex has been optimized without imposing any symmetry constraints. For the heavy metal Nb, the valence electrons have been described by double numerical basis set with polarization (DNP) [43] function and the core electrons are described with local pseudo-potential (VPSR) [45,46] which accounts for the scalar relativistic effect expected to be significant for heavy metal elements. Frequency calculation has been performed on the optimized geometry of the complex and is found to be positive, confirming the structure to be at energy minima.

3.3 Results and discussion

3.3.1 Synthesis

The water soluble polymers are essentially polychelatogens with functional groups capable of forming co-ordinate bonds with metal ions [27]. It is therefore often possible to synthesize soluble macro complexes by transposing synthetic protocols

usually employed for preparing their monomeric analogues. Synthesis of soluble niobium(V) compounds is considered to be rather challenging owing to very low solubility of the common Nb containing starting materials [4]. In the current study, water soluble $Na_3[Nb(O_2)_4]\cdot 13H_2O$ has been used as precursor complex, which was prepared by a reported method [41].

The synthesis of the soluble macrocomplexes, **3.1** and **3.2** were achieved by reacting the precursor complex with the respective WSP in presence of excess of 30% H_2O_2 in an aqueous medium**.** Polymers such as poly(acrylate) and poly(styrene sulfonate) have pH dependent solubility and have been used to prepare catalytically active complexes that can be dissolved by adjusting the pH of a solution. The mode and extent of chelation of the pendant ligand groups *viz.*, carboxylate and sulfonate, of these polymers are also known to be sensitive to pH. For the present synthesis, pH of 5 was found to be optimal for the formation of triperoxoniobium species and their anchoring to the pendant ligand groups of the respective polymers leading to the desired synthesis. The other essential component of the synthetic methodology included maintenance of required time and temperature at $\leq$ 4 °C. The supported complexes were finally isolated as white microcrystalline solids by inducing precipitation with acetone, which is an effective and general way of isolating soluble polymers. The compound was observed to be stable in solid state for several weeks, when stored dry at < 30 °C.

3.3.2 Characterization

The elemental analysis data of the macrocomplexes **3.1** and **3.2**, (**Table 3.1**) indicated the presence of three peroxide moieties per metal centre. The loading on the compounds based on the elemental analysis and confirmed by EDX analysis are presented in **Table 3.1**. The niobium loading on the compounds, **PANb (3.1)** and **PSSNb (3.2)** correspond to 2.08 and 1.62 mmol per gram of the polymeric support, respectively which was calculated on the basis of Nb content, obtained from elemental analysis and confirmed by EDX spectral analysis as well as with inductively coupled plasma optical emission spectrophotometer (ICP-OES). The pNb compounds were diamagnetic in nature, as was evident from the magnetic susceptibility measurement consistent with the presence of Nb centers in their +5 oxidation states.

3.3.2.1 SEM and Energy Dispersive X-ray (EDX) analysis

Scanning Electron micrographs (SEM) of the pristine polymers and the respective supported Nb complex, were recorded in order to understand the morphological changes occurring on the surface of the polymer after loading of the pNb species to the polymer matrix. Comparison of these images showed that the smooth surfaces of the parent polymer, PA as well as PSS have been distinctly altered after incorporation of the peroxometallates to the polymers. That the metal ions are distributed across the surface of the polymeric complex was evident from the significant roughening of the surface of **PANb** (**3.1)** and **PSSNb (3.2)** [**Fig. 3.1(b)** and **3.1(d)**, respectively]. Energy dispersive X-ray spectroscopic analysis, which provides *in situ* chemical analysis of the bulk, was carried out by focusing on multiple regions over the surface of the polymer incorporated pNb compounds. EDX data clearly showed Nb, Na, C and O as the constituents of the compound **PANb** (**3.1).** Moreover, the presence of S in addition to Nb, Na, C and O in the compound **PSSNb** (**3.2)** was confirmed from the EDX analysis (**Fig. 3.2**). The results presented in **Table 3.1** for each of the compounds are the average of the data from these regions. The composition of the compounds derived from the EDX analysis agreed well with the elemental analysis values (**Table 3.1**).

3.3.2.2 IR and Raman spectral studies

The FTIR and Raman spectra of the complexes, **PANb** (**3.1)** and **PSSNb** (**3.2)**, presented in **Fig. 3.3 - Fig. 3.6**, and the significant spectral features summarized in **Table 3.2** indicated the successful anchoring of the pNb species to the respective polymer chain, by displaying the expected spectral pattern. In contrast to the IR spectrum of the starting tetraperoxoniobate complex (**Fig. 4.2**) which showed a single peak at 815 cm^{-1} corresponding to ν(O-O) vibration, the spectra of **3.1** and **3.2** clearly showed the presence of triperoxoniobium species in these complexes by exhibiting three typical absorptions in the 800 - 860 cm^{-1} range attributable to ν(O-O) modes of the triperoxoNb moiety [4]. In addition, the ν_{as}(Nb-O_2) and ν_s(Nb-O_2) vibrations were observed as expected in the 500-600 cm^{-1} [4,47]. The IR results have been substantiated further by complementary Raman spectrum for each of the compounds.

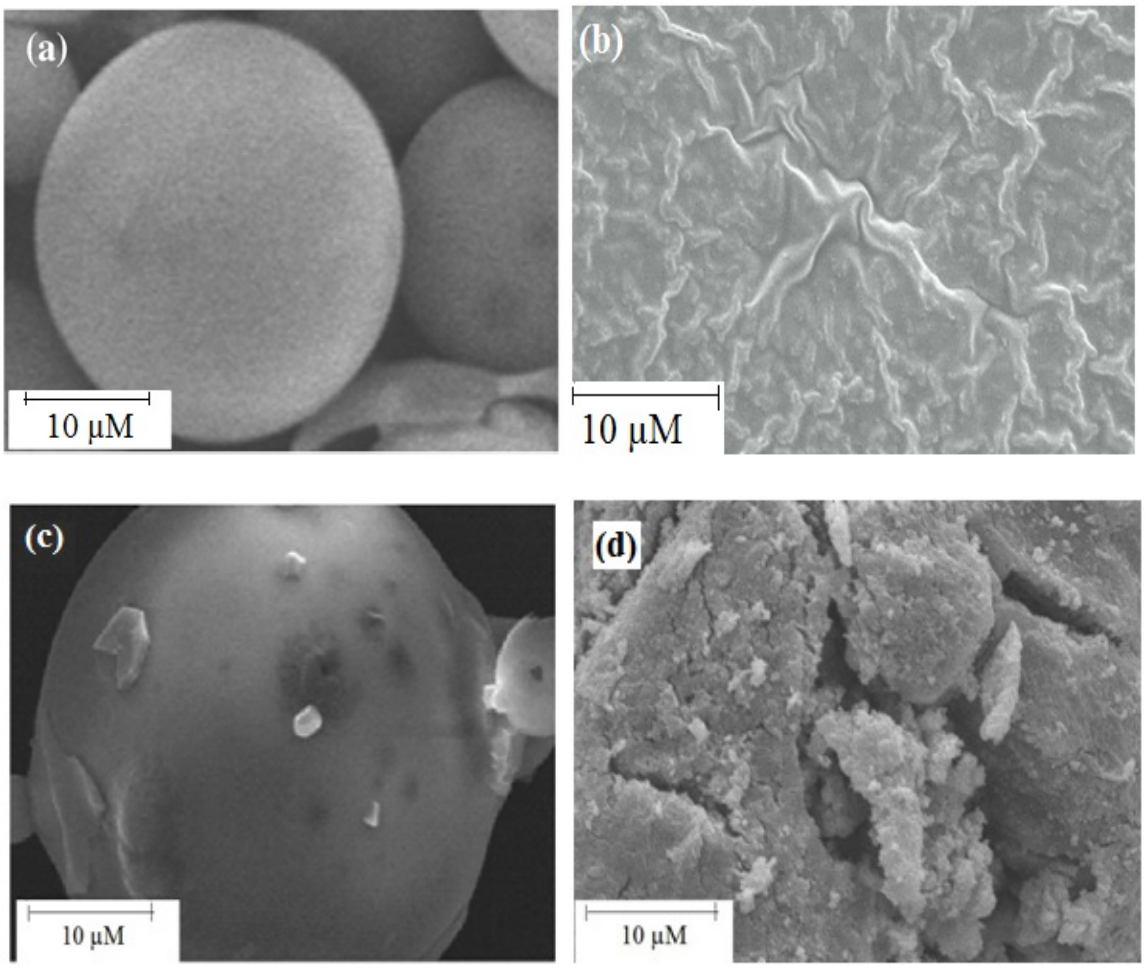

Fig. 3.1 Scanning electron micrographs of (a) PA, (b) **PANb (3.1)** and (c) PSS, (d) **PSSNb (3.2)**.

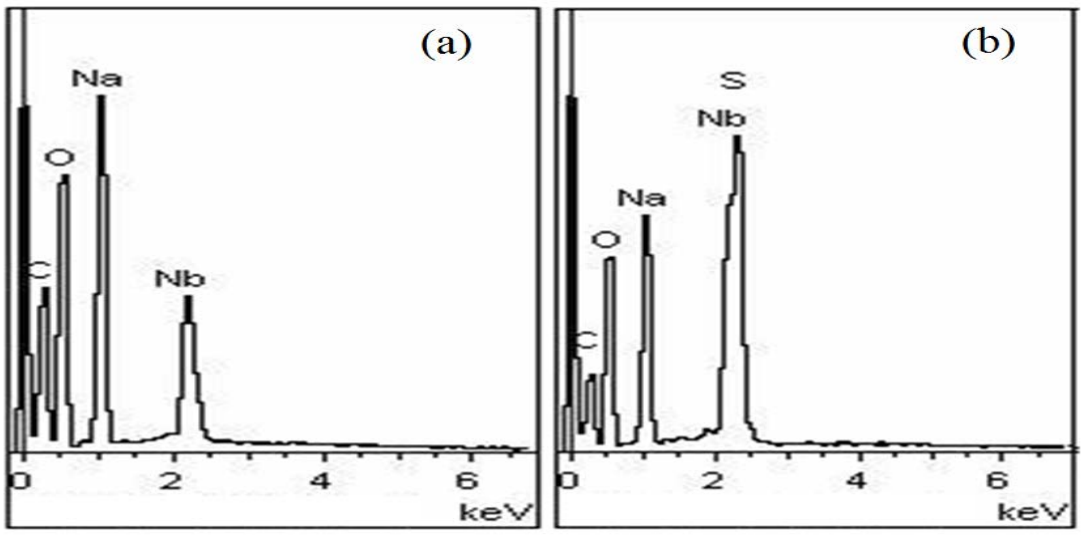

Fig. 3.2 EDX spectra of (a) **PANb (3.1)** and (b) **PSSNb (3.2)**.

Table 3.1 Analytical data for the polymer-bound peroxoniobate compounds

Compound	% found from elemental analysis (% obtained from EDX spectra)						Nb: O_2^{2-}	Metal-ion loading[b] (mmol g^{-1})
	C	H	Na	S	Nb	O_2^{2-}		
PANb	20.75	1.89	17.97	-	19.31[a]	20.30	1:3.05	2.08
	(20.81)		(17.99)		(19.27)		1:3.06	2.07
PSSNb	30.06	2.20	11.09		15.06[a]	15.53	1: 2.99	1.62
	(30.39)		(10.97)	(6.59)	(14.99)		(1:3.01)	(1.61)

[a]Obtained from ICP

[b]Niobium loading $= \frac{\text{Observed metal \% X 10}}{\text{Atomic weight of metal}}$

For the carboxylato coordination, the difference of wave number $\Delta v = v_{as}$-v_s relationship has been used as one of the criteria for the assignment of the mode of carboxylate binding to a metal centre [48]. The criterion is also applicable to polycarboxylates as well as poly(acrylates) [20]. In the spectrum of **3.1** (**Fig. 3.3** and **Fig. 3.4**), the v_{as}(COO) and v_s(COO) modes are observed at 1571 and 1408 cm^{-1}, respectively whereas, in the pristine polymer PA in the v_{as}(COO) occurs at 1565 and the v_s(COO) at 1409 cm^{-1}. The observed Δv (163 cm^{-1}) in case of the **3.1** which remains close to that observed for free PA, is characteristic of a bridging bidentate coordination pattern of the carboxylate group. The Raman spectrum showed the corresponding peaks at 1552 and 1411 cm^{-1} for v_{as}(COO) and v_s(COO) modes respectively. The presence of free COOH groups in the compound was also evident from an additional IR band appearing at 1710 cm^{-1}. The weak intensity bands observed in the far-IR region in the vicinity of 500 and 400 cm^{-1} have been assigned to metal oxygen vibrations.

The spectrum also showed the presence of lattice water in the pNb compound by displaying strong and broad v(OH) absorptions at 3500-3400 cm^{-1}. The strong absorbance observed at 2925 cm^{-1} in the Raman spectrum (**Fig. 3A.1**), which appears as a medium intensity IR band at 2939 cm^{-1} has been ascribed to C-H stretching vibration.

In the spectrum of the pure polymer PSS, the bands at 1197 cm^{-1} and 1039 cm^{-1} represent S-O stretching for asymmetric and symmetric absorption bands of SO_2, respectively [49,50]. In the spectrum of the complex **3.2** (**Fig. 3.5** and **Fig. 3.6**), a broad band with distinct absorptions at 1217 and 1181 cm^{-1}, in addition to symmetric vibration of S-O at 1033 cm^{-1}, appeared which may be ascribed to the splitting of S-O stretching vibrations originating from complexed sulfonate group [49,51-53]. The spectrum of the compound exhibited characteristic absorptions at *ca.* 1637 and 1499 cm^{-1} due to its phenyl group and bending CH_2, respectively [49,51,54]. Additional characteristic features for the complex **3.2** are at 813, 827 and 846 cm^{-1} which can be assigned for v(O-O) that shows the presence of three peroxo groups. The peaks at 550 and 489 cm^{-1} bands were observed for v_{as}(Nb-O_2) and v_{sym}(Nb-O_2) vibrations, respectively. Appearance of strong absorptions showed at 3500-3400 cm^{-1} indicated the presence of lattice water in the complex.

In the Raman spectra for **3.2** (**Fig. 3.6**), peaks at 812, 841, 859 cm^{-1} were observed which can be assigned for ν(O-O) and the bands at 543 and 471 cm^{-1} were assigned for ν_{as}(Nb-O_2) and ν_s(Nb-O_2) vibrations, respectively. Additionally, the spectra of the complex **3.2** show asymmetric bands of SO_2 at 1210 and 1148 cm^{-1} as well as symmetric vibration of S-O at 1028 cm^{-1} that can be attributed to complexed sulfonate.

Table 3.2 Experimental and theoretical infrared and Raman spectral data (cm^{-1}) for **PANb** (**3.1)** and **PSSNb (3.2)**[a]

Assignment			**PANb**	**PSSNb**
ν(O-O)	IR	Exp.	813(s), 826(sh), 846(m)	813(s), 827(m), 846(sh)
		Calc.	825, 842, 884	797, 828, 844
	R	Exp.	809(sh), 824(m), 840(s)	812(sh), 841(m), 859(s)
		Calc.	825, 839, 877	828, 844, 916
ν_{as}(Nb-O_2)	IR	Exp.	593(m)	550(s)
		Calc.	587	570
	R	Exp.	533(s)	543(s)
		Calc.	547	555
ν_s(Nb-O_2)	IR	Exp.	549(s)	489(m)
		Calc.	547	488
	R	Exp.	470(sh)	471(m)
		Calc.	477	442
ν_a(COO)	IR	Exp.	1571(s)	---
		Calc.	1577	
	R	Exp.	1552(vw)	
		Calc.	1577	
ν_s(COO)	IR	Exp.	1408(m)	---
		Calc.	1397	
	R	Exp.	1411(m)	
		Calc.	1412	
ν_{as}(S-O)	IR	Exp.	---	1217(sh), 1181(s)
		Calc.		1249, 1175
	R	Exp.	---	1210(m), 1148(s)
		Calc.		1250, 1177

[a]s, strong; m, medium; vw, very weak; sh, shoulder

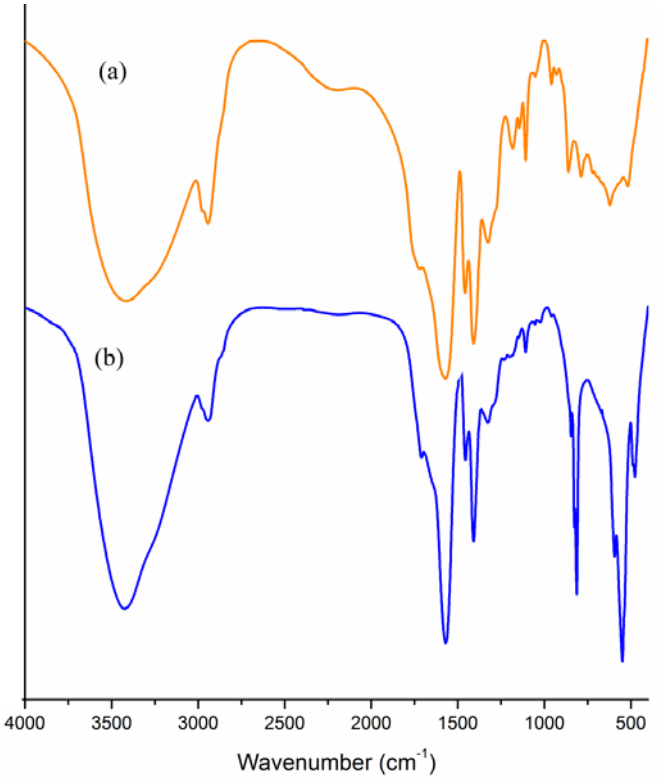

Fig. 3.3 IR spectra of (a) PA and (b) **PANb**.

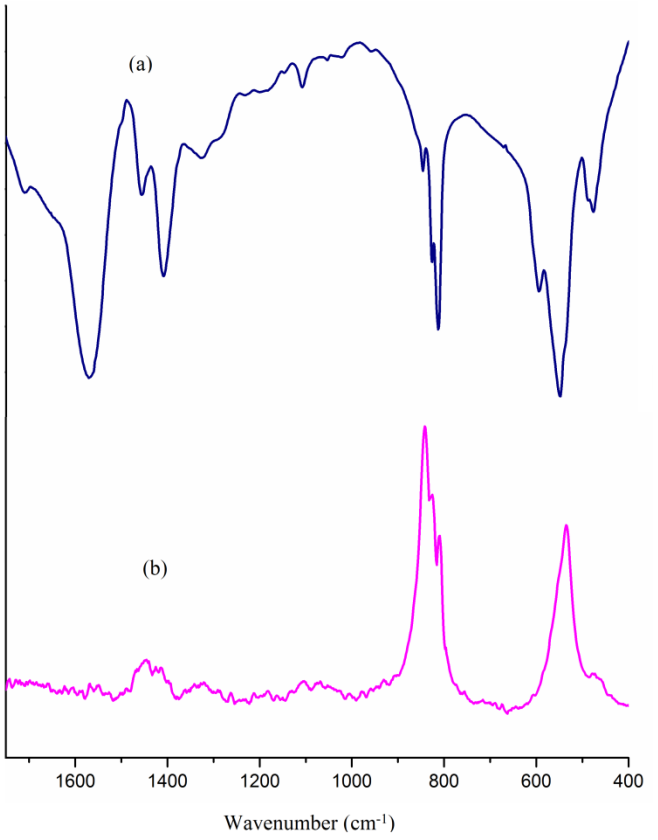

Fig. 3.4 (a) IR & (b) Raman spectra of **PANb**.

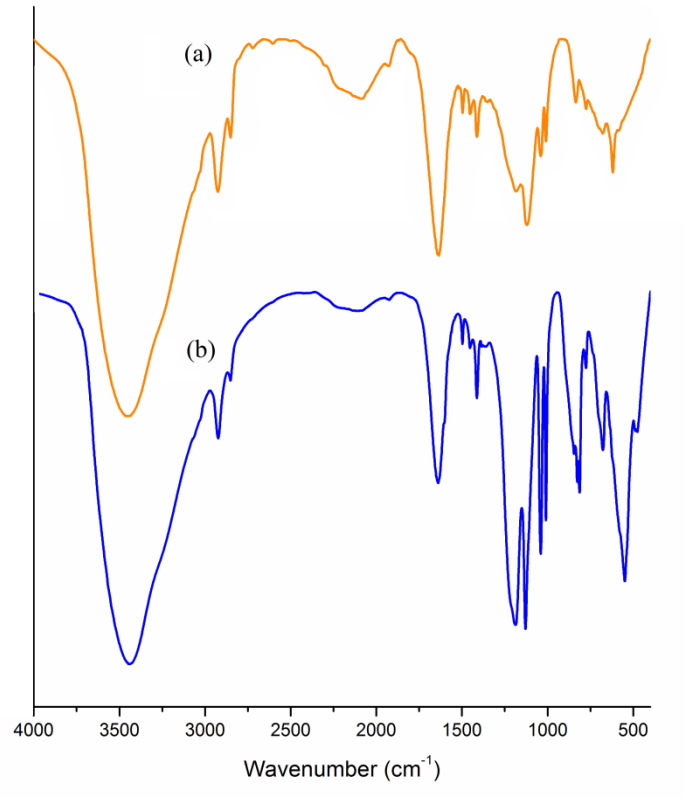

Fig. 3.5 IR spectra of (a) PSS and (b) **PSSNb**.

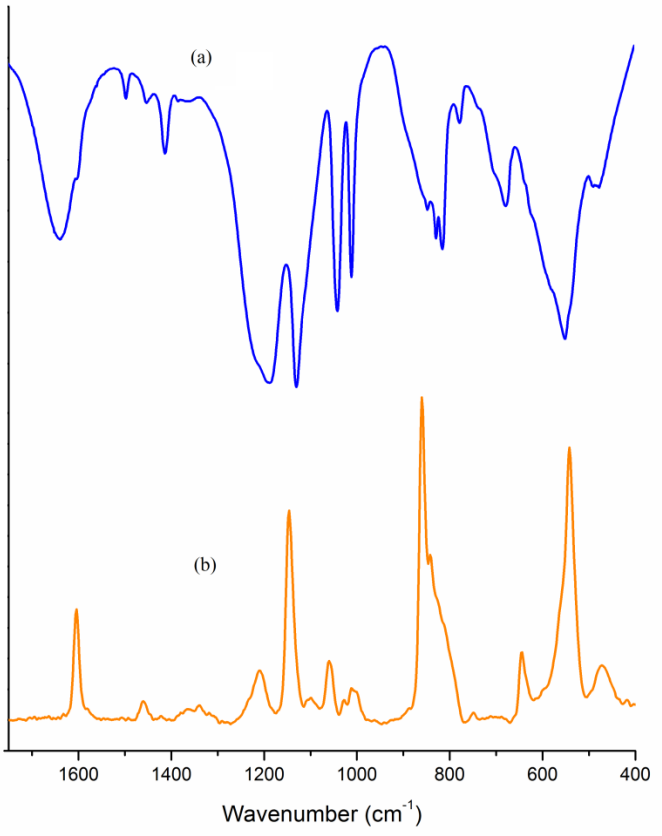

Fig. 3.6 (a) IR & (b) Raman spectra of **PSSNb**.

3.3.2.3 TGA-DTG analysis

The TGA-DTG profile of the poly(acrylate) and poly(styrene sulfonate) bound pNb compounds (**Fig. 3.7** and **Fig. 3.8**), revealed that the compounds undergo gradual decomposition on heating up to a final temperature of 700 °C. It is notable that unlike some other peroxometal compounds the title compounds did not explode on heating. The first stage of decomposition, with the liberation of lattice water molecules, occurs in the temperature ranges of 40-113 °C and 40-105 °C for the complexes **PANb (3.1)** and **PSSNb (3.2)**, respectively. The subsequent decomposition stage has been observed in the range of 137-251 °C in case of **3.1** and 126-222 °C for **3.2**, which may be ascribed to the loss of peroxo groups from the complexes. The absence of peroxide group in the decomposition product, isolated at this stage, was also verified by its IR spectrum. On further increasing the temperature, the decomposition corresponding to decarboxylation and breakdown of the polymer chain was observed in the temperature range of 359-552 °C for the complex, $Na_3[V_2O_2(O_2)_4$(carboxylate)]-PA (**PAV**) [19]. As expected, the thermal decomposition pattern of **PANb** agreed well with TGA patterns exhibited by the corresponding peroxovanadate [19], and peroxomolybdenum containing analogues reported previously [20].

In case of **3.2**, after the initial dehydration and loss of peroxo groups, a two stage decomposition in the range of 370-613 °C, which is possibly due to loss of the sulfonate group and rupturing of polymers occurs. By analogy with the TGA data available for poly(vinyl sulfonate) and these decompositions in the range of 370-493 °C and 503-613 °C, have been ascribed to loss of sulfonate group and rupturing of the polymer accompanied by evolution of ethylene, water, SO_2 and CS_2 [55]. The total weight loss which occurred during the course of the overall decomposition process *viz.* loss of lattice water, coordinated peroxide and polymeric functional, on heating the compound up to a final temperature of 700 ^oC was recorded to be 40.5% for **PANb (3.1)** and 36.8% for **PSSNb (3.2)**.

After the complete degradation of the pNb macrocomplexes, the remaining residue was subjected to IR spectral analysis. The residue was confirmed to be an oxoniobate species as indicated by its IR spectrum which showed the typical Nb=O stretching at 881 and 833 cm^{-1} [56]. An additional band observed at 1441 cm^{-1} in the IR

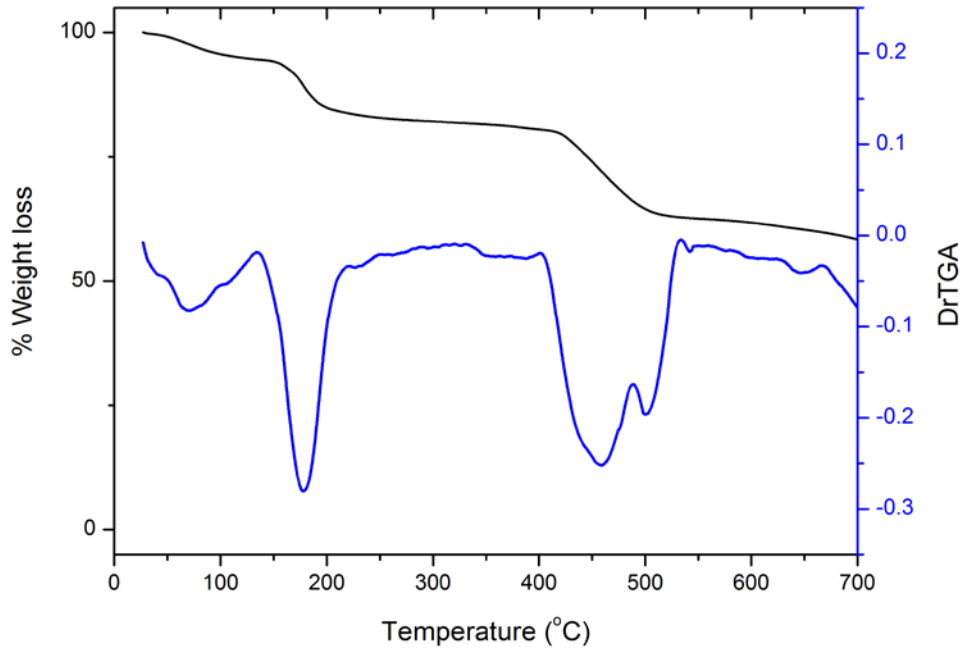

Fig. 3.7 TGA-DTG plots of **PANb**.

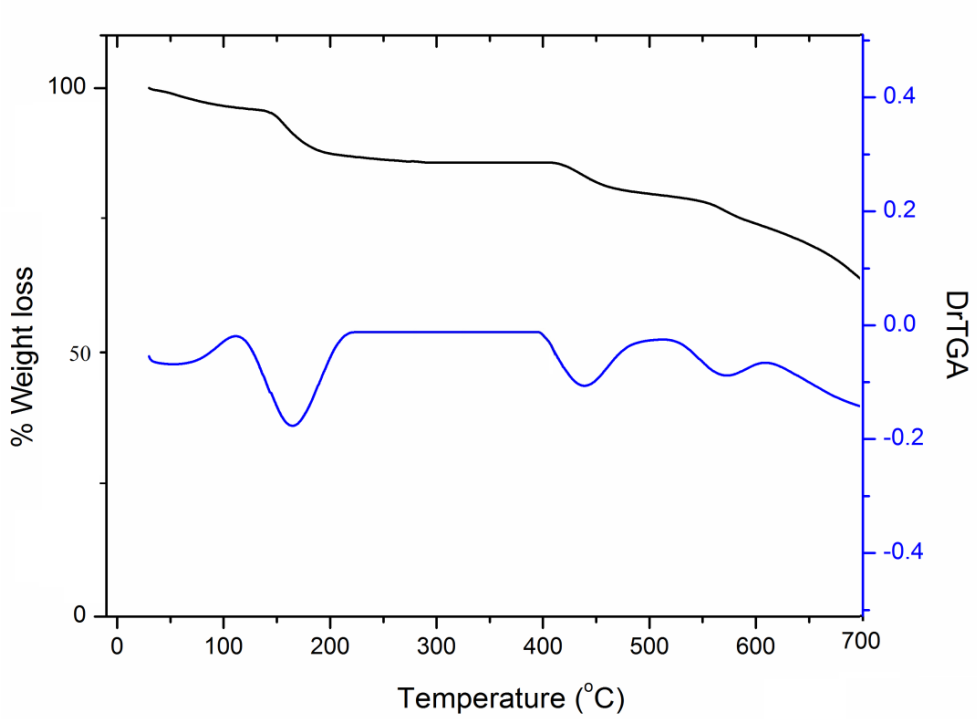

Fig. 3.8 TGA-DTG plot of **PSSNb**.

spectrum is attributable to sodium carbonate present in the residue along with oxoniobate species for **PANb (3.1)** (**Fig. 3A.2**). Thermal decomposition of poly(sodium acrylate) has been reported to produce sodium carbonate along with the release of CO_2 and CO as final degradation products [57]. The findings from the TGA-DTG analysis furnished additional evidence in support of the composition and formula assigned to the macrocomplexes, **3.1** and **3.2**.

3.3.2.4 ^{13}C and ^{93}Nb NMR studies

Crucial information regarding the bonding pattern of the macromolecular ligands to the metal centers in the compounds can be drawn from ^{13}C NMR data. The ^{13}C NMR spectrum of neat poly(acrylate) (**Fig. 3.9a**) displays typical resonances corresponding to chain carbon atoms of CH_2 and CH groups at 36.04 and 45.75 ppm, respectively in addition to the signal due to the carboxylate carbon atoms centered at 184 ppm (**Table 3.3**). In the spectrum of polymeric complex **3.1** (**Fig. 3.9b)**, an additional new peak at a considerably lower field of 215 ppm appeared which has been assigned to the carbon atom of the complexed carboxylate group, on the basis of the available literature [20,58]. The substantial downfield shift, $\Delta\delta$ ($\delta_{complex}$ - $\delta_{free\ carboxylate}$) ≈ 31 ppm in the case of PA-bound compound relative to the free carboxylate peak, is in close agreement with the values obtained previously in case of other poly(acrylate) bound peroxometallates including **PAV** [20], and is an indication of strong metal ligand interaction. Furthermore, the appearance of the resonance at 215 ppm as a singlet, revealed a single carbon environment for the co-ordinated carboxylate group, thereby testifying to the presence of only one complex species in solution.

In the ^{13}C NMR spectrum of compound **3.2** (**Fig. 3.10b**), peaks due to poly(sodium styrene sulfonate) matrix remained practically unaffected by complexation as compared to the pure polymer (**Fig. 3.10a**) and the data are represented in the **Table 3.3**. This is not unexpected keeping in view that Nb(V) atom is bound to the polymer through the sulfonate groups and hence is well separated from the chain as well as ring carbon atoms of the polymer support.

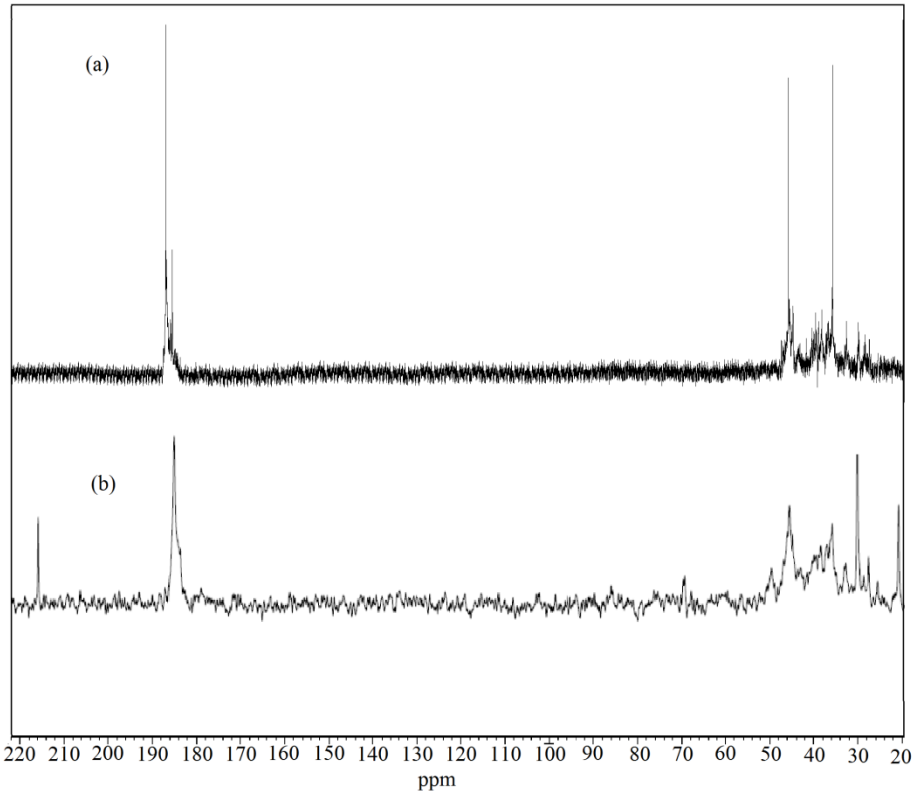

Fig. 3.9 ^{13}C NMR spectra of (a) PA and (b) **PANb** in D_2O.

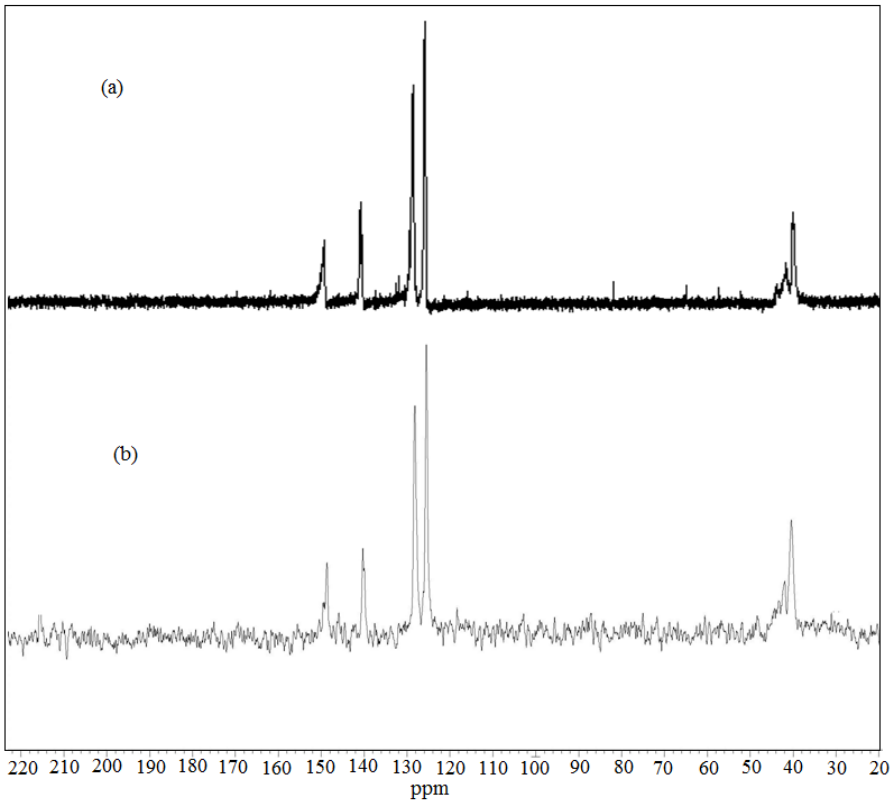

Fig. 3.10 ^{13}C NMR spectra of (a) PSS and (b) **PSSNb** in D_2O.

Table 3.3 ^{13}C NMR spectral data for **PANb** and **PSSNb**

	Chemical shift (ppm)									
	Carboxylate carbon				Ring carbon					
Compound	Free	Complexed	CH	CH_2	C1	C2	C3	C4	C5	C6
PA	184.50		45.52	36.10						
PANb	184.76	215.47	45.75	36.04						
PSS	-	-	40.52	44.14	140.35	128.84	125.57	148.55	125.35	128.17
PSSNb	-	-	40.44	43.26	140.31	128.18	125.52	148.66	125.25	127.76

Further information regarding the nature of the complexes in solution was derived from ^{93}Nb-NMR studies (**Fig. 3.11**). The assignment of the peaks in the present study was on the basis of available data [59]. Being the only magnetically active isotope of niobium, ^{93}Nb has several beneficial NMR properties, including the high magnetogyric ratio and the 100% natural abundance, which makes ^{93}Nb one of the most NMR receptive nuclei [60]. Thus, ^{93}Nb NMR is a promising technique to study the local environment of niobium. In an extensive study of ^{93}Nb solid state NMR of niobate compounds by Lapina *et al.* [59], it has been demonstrated that the ^{93}Nb NMR chemical shift is sensitive to the co-ordination number of Nb sites. Identifying several common ^{93}Nb NMR features, they proposed a chemical shift scale based on niobium co-ordination number. It has been depicted that 7 and 8 co-ordinated Nb sites exhibit high-field shift compared to 6 co-ordinated Nb. In the present study, in the NMR spectrum of macro complexes, **3.1** and **3.2,** a single resonance at -1530 ppm and -1537 ppm, respectively (**Fig. 3.11b** and **Fig. 3.11c**), was observed whereas, in case of the sodium tetraperoxoniobate species the peak occurred at a slightly lower field at -1481 ppm (**Fig. 3.11a**). These values are within the range that corresponds to an eight co-ordinated

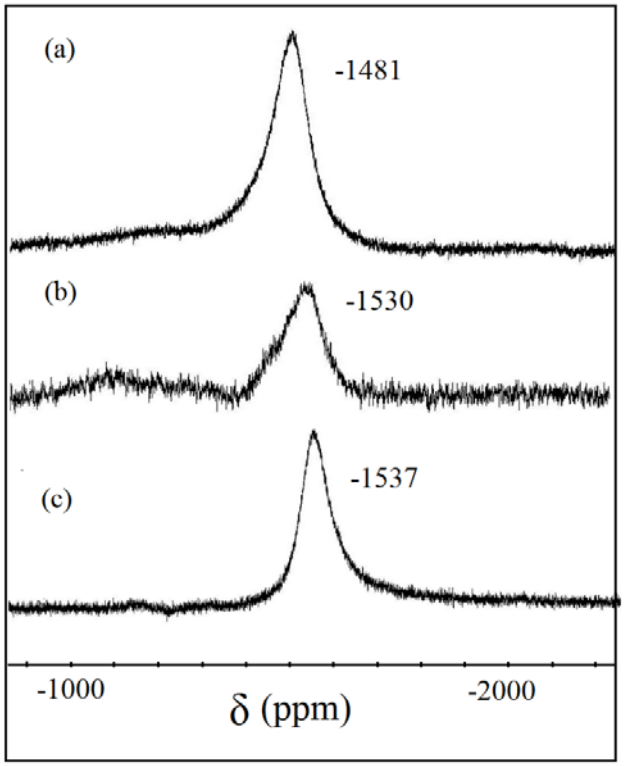

Fig. 3.11 ^{93}Nb NMR spectra of 0.2 mM solution of (a) **NaNb,** (b) **PANb** and (c) **PSSNb** in D_2O.

environment for Nb, consistent with the formula assigned to these compounds. Slight variation in resonance positions are likely due to the difference of the ligand environment between the complexes examined, resulting from the presence of co-ordinated carboxylate groups in **3.1** and sulfonate coordination in **3.2**. It has already been reported by Flambard *et al.* [61] that apart from coordination number, ^{93}Nb NMR chemical shift is also influenced by the local charge on Nb. Existence of Nb(V) in the compounds **NaNb, PANb (3.1)** and **PSSNb (3.2)** in a single co-ordination environment was further confirmed from the identification of a single peak in the spectrum.

The structures envisaged for the macro complexes, **PANb (3.1)** and **PSSNb (3.2)**, on the basis of the above collective evidence are shown schematically in **Fig. 3.12**. The structure is comprised of Nb(V) atom with three side-on bound peroxo groups, bonded to the polymer chain *via* its pendant carboxylate groups in a bridged bidentate manner for

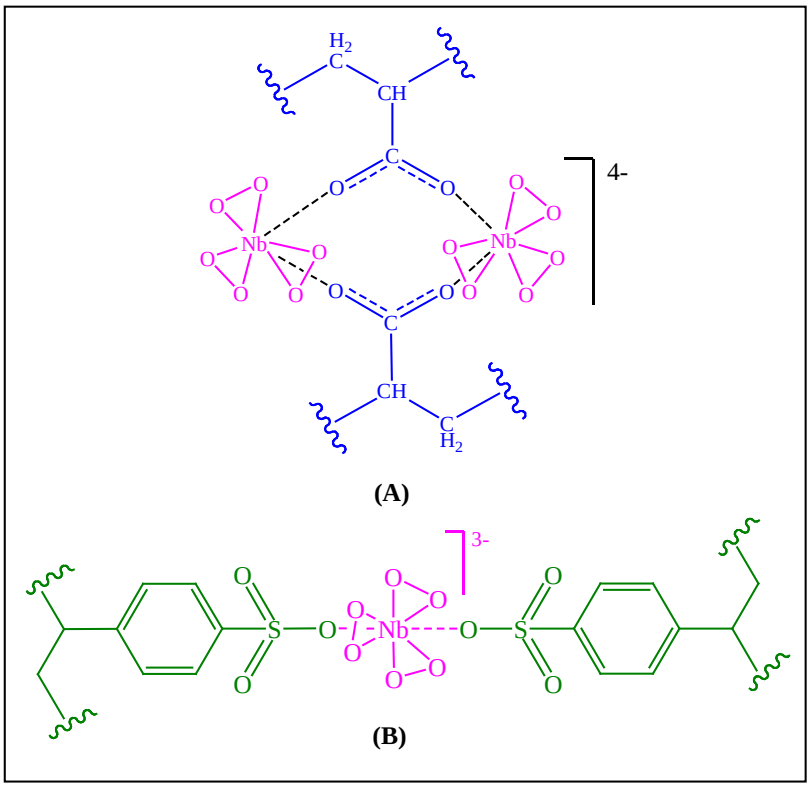

Fig. 3.12 Proposed structures of soluble polymer anchored pNb complexes, (A) **PANb (3.1)** and (B) **PSSNb (3.2)**. **PA** = poly(sodium acrylate)**, PSS** = poly(sodium styrene sulfonate) and "〰" represents polymer chain.

3.1. It is notable that similar modes of carboxylate co-ordination were also observed previously in cases of poly(acrylate) anchored peroxo compounds of V and Mo [19,20]. It is reasonable to expect that in the polymer-anchored complexes the inter chain interaction between the dinuclear peroxometal centers and the neighbouring pendant carboxylate groups of the polymer chains would provide additional support to the carboxylate-bridged triperoxo metal moieties by completing eight-fold coordination around each Nb centre. The structure of the complex **3.2** includes an eight co-ordinated Nb with two unidentate sulfonate groups and three side-on-bound η^2-peroxo moieties. It is worthy to note that in the structurally characterized pNb compounds reported so far, the niobium atom consistently displayed a co-ordination number of eight [4].

3.3.2.5 Density functional studies

We have verified the viability of the structure proposed for the poly(acrylate) bound pNb complex **PANb (3.1)** and poy(styrene sulfonate) anchored pNb complex **PSSNb (3.2)**, using density functional theory (DFT) method [42,43]. The initial structures of the macro complexes have been modelled on the basis of experimentally derived structural information. For **PANb (3.1)**, a model complex has been generated representing a section of each of the polymers, consisting of three repeating units of the polymer with one dinuclear peroxo niobium moiety bonded through bridging carboxylate groups of two polymer chains. The optimized geometry of the **3.1** is presented in **Fig. 3.13** which shows two Nb(V) centres, each bonded to three η^2-peroxo groups and O atoms of the bridging carboxylate groups being in *trans* configuration. In the case of the complex **PSSNb** (**3.2**), the optimized geometry given in **Fig. 3.14** shows that the central metal atom (Nb) is coordinated to six oxygen atoms of three η^2-peroxo groups and the remaining two sites are bonded to oxygen atoms from the two pendant sulfonate groups of poly(styrene) chains in a *trans* configuration.

Absence of imaginary frequency in the vibrational frequency calculations for each of the model complexes suggested that the complexes represent a stable structure. Co-ordination polyhedron around each of the eight co-ordinated Nb(V) centres in the compounds can be described as a dodecahedron. The observation is consistent with the structures of the majority of the reported peroxoniobium complexes [4,8-11,41]. The selected geometrical parameters such as bond angle and bond length obtained for the

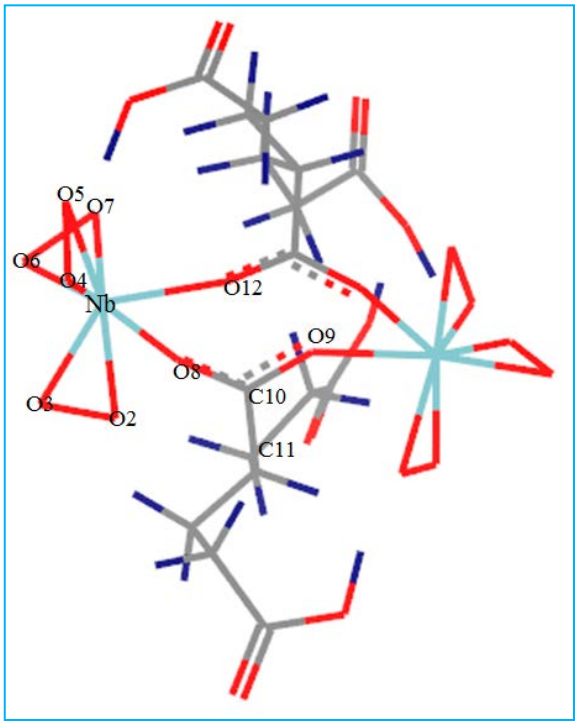

Fig. 3.13 Optimized geometry of **PANb** complex obtained by using density functional theory (DFT). The numerical numbers represent the labeling of the atoms as in **Table 3.4**. (Colors: light blue is niobium, red is oxygen, grey is carbon and dark blue lines represent hydrogen).

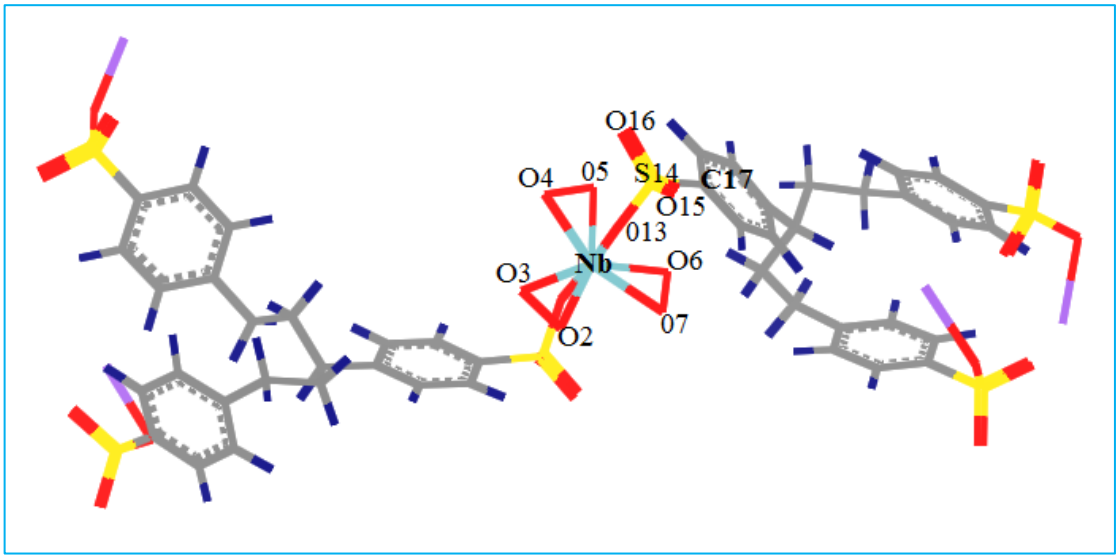

Fig. 3.14 Optimized geometry of **PSSNb** complex obtained by using density functional theory (DFT). The numerical numbers represent the labeling of the atoms as in **Table 3.4**. (Colors: light blue is niobium, red is oxygen, yellow is sulfur, grey is carbon, dark blue is hydrogen and purple lines represent sodium).

complexes from the DFT calculations, correlated well with the available crystallographic parameters pertaining to heteroleptic pNb complexes (**Table 3.4**) [4,8-11,41]. Furthermore, calculated IR and Raman data for the optimized geometry presented in **Table 3.2** was observed to be in good agreement with the experimentally determined vibrational frequencies. Thus the mutually consistent results of theoretical calculations and experimental findings lend further credence to the proposed geometries of the complexes, **PANb (3.1)** and **PSSNb (3.2)**.

Table 3.4 Selected bond lengths (Å) and bond angles (degree) for **PANb** and **PSSNb** complexes calculated using density functional theory (DFT) as implemented in the $DMol^3$ package

Structural index[a]	**PANb**	Structural index[a]	**PSSNb**
Nb-O2	2.046	Nb-O2	2.171
Nb-O3	2.032	Nb-O3	2.167
Nb-O4	1.988	Nb-O4	2.159
Nb-O5	1.986	Nb-O5	2.166
Nb-O6	2.017	Nb-O6	2.178
Nb-O7	2.051	Nb-O7	2.171
Nb-O8	2.171	Nb-O13	2.132
O2-O3	1.457	O2-O3	1.367
O4-O5	1.454	O4-O5	1.367
O6-O7	1.455	O6-O7	1.361
C10-O8	1.279	S14-O13	1.558
C10-O9	1.262	S14-O15	1.486
C10-C11	1.496	S14-O16	1.487
∠O2-Nb-O3	42.6	S14-C17	1.740
∠O4-Nb-O5	42.3	∠O2-Nb-O3	36.85
∠O6-Nb-O7	42.3	∠O4-Nb-O5	36.58
∠O8-Nb-O12	74.1	∠O6-Nb-O7	36.62

[a]See **Fig. 3.13** for **PANb** and **Fig. 3.14** for **PSSNb,** for atomic numbering.

3.4 Conclusion

In summary, we have achieved the synthesis of a pair of novel water soluble and structurally defined niobium containing macro complexes by anchoring pNb species to linear water soluble polymer matrices. The compounds were characterized by spectroscopic and other conventional methods, including ^{93}Nb NMR and SEM-EDX analysis. Spectral and chemical analysis data for the compounds, substantiated by DFT calculation data, provided unambiguous evidence for the composition of the ligand sphere and possible mode of co-ordination of the pendant functional groups of the polymers to the Nb(V) centre.

Results of investigations on the catalytic activity of these macrocomplexes in organic oxidation, as well as the findings on some of their bio-relevant properties are described in Chapters 5-8 of the thesis.

Appendix: 3A

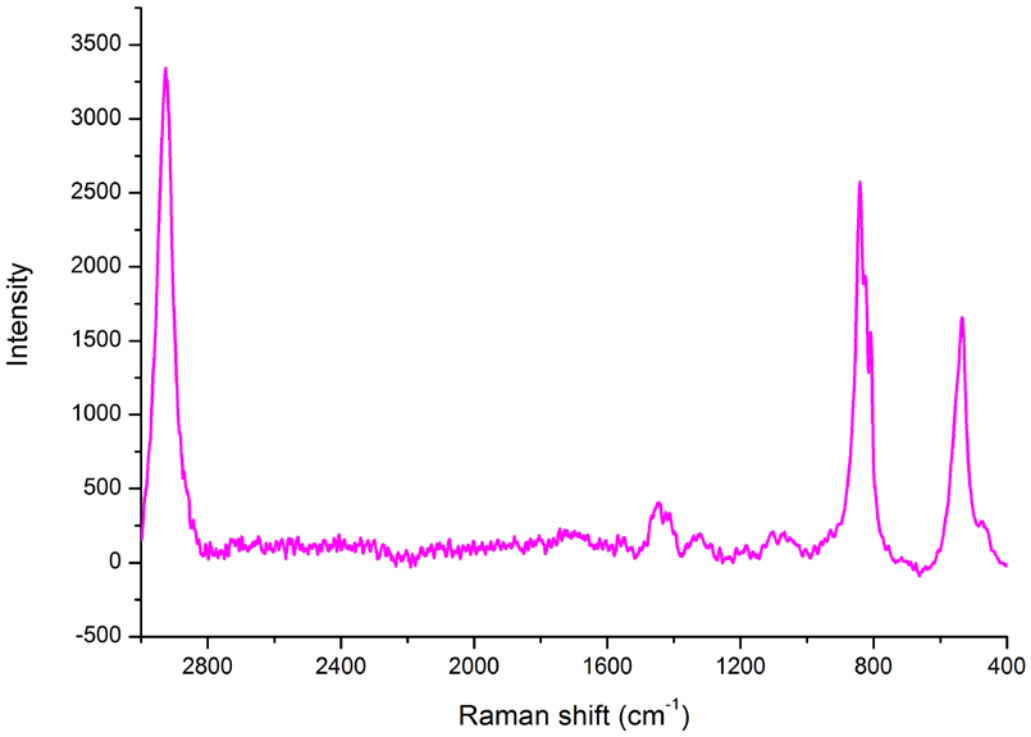

Fig. 3A.1 Raman spectrum of **PANb**.

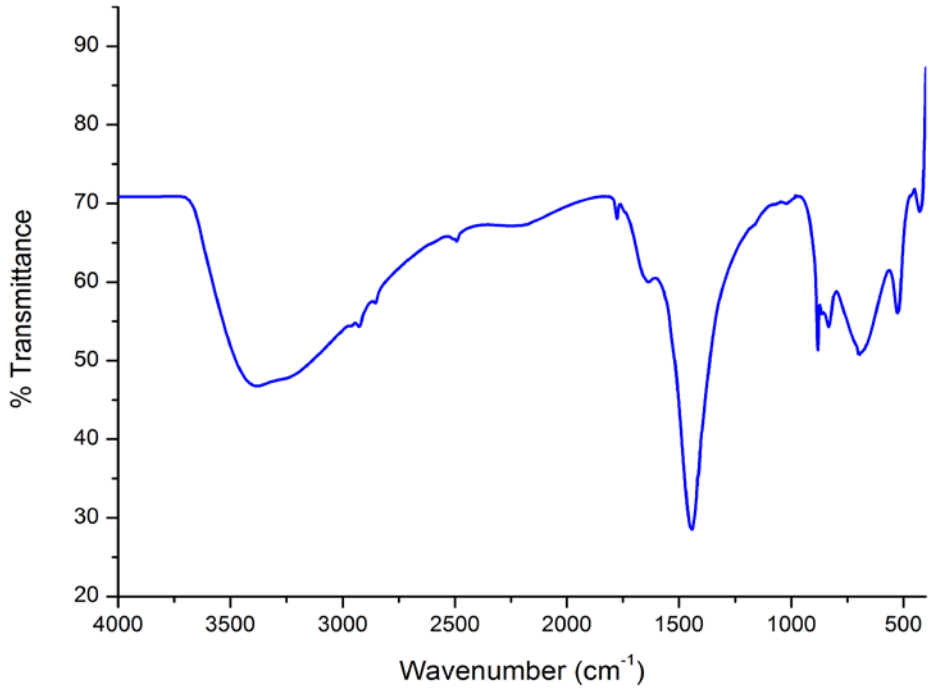

Fig. 3A.2 IR spectrum of the residue after TGA of **PANb** up to 700 °C.

References

1. Ajjou, A. N. and Alper, H. A new, efficient, and in some cases highly regioselective water-soluble polymer rhodium catalyst for olefin hydroformylation. *Journal of the American Chemical Society*, 120(7):1466-1468, 1998.
2. Yan, Y., Zhang, J., Ren, L., and Tang, C. Metal-containing and related polymers for biomedical applications. *Chemical Society Reviews*, 45(19):5232-5263, 2016.
3. Macromolecules containing metal and metal-like elements. In Abd-El-Aziz, A. S., Carraher, C. E., Pittman, C. U., Sheats, J. E., and Zeldin, M., editors, *Biomedical Applications*, page 3:6, John Wiley & Sons Inc., Canada, 2004.
4. Bayot, D. and Devillers, M. Peroxo complexes of niobium(V) and tantalum(V). *Coordination Chemistry Reviews*, 250(19):2610-2626, 2006.
5. Chen, C., Yuan, H., Wang, H., Yao, Y., Ma, W., Chen, J., and Hou, Z. Highly efficient epoxidation of allylic alcohols with hydrogen peroxide catalyzed by peroxoniobate-based ionic liquids. *ACS Catalysis*, 6(5):3354-3364, 2016.
6. Thomadaki, H., Lymberopoulou-Karaliota, A., Maniatakou, A., and Scorilas, A. Synthesis, spectroscopic study and anticancer activity of a water-soluble Nb(V) peroxo complex. *Journal of Inorganic Biochemistry*, 105(2):155-163, 2011.
7. Maniatakou, A., Karaliota, S., Mavri, M., Raptopoulou, C., Terzis, A., and Karaliota, A. Synthesis, characterization and crystal structure of novel mononuclear peroxotungsten(VI) complexes. Insulinomimetic activity of W(VI) and Nb(V) peroxo complexes. *Journal of Inorganic Biochemistry*, 103(5):859-868, 2009.
8. Maniatakou, A., Makedonas, C., Mitsopoulou, C. A., Raptopoulou, C., Rizopoulou, I., Terzis, A., and Karaliota, A. Synthesis, structural and DFT studies of a peroxo-niobate complex of the biological ligand 2-quinaldic acid. *Polyhedron*, 27(16):3398-3408, 2008.
9. Bayot, D., Degand, M., Tinant, B., and Devillers, M. Spectroscopic and structural characterizations of water-soluble peroxo complexes of niobium(V) with N-containing heterocyclic ligands. *Inorganica Chimica Acta*, 359(5):1390-1394, 2006.
10. Bayot, D., Tinant, B., Mathieu, B., Declercq, J. P., and Devillers, M. Spectroscopic and structural characterizations of novel water-soluble peroxo [polyaminocarboxylatobis(N-oxido)]niobate(V) complexes. *European Journal of Inorganic Chemistry*, 2003(4):737-743, 2003.

11. Bayot, D., Tinant, B., and Devillers, M. Homo-and heterobimetallic niobium V and tantalum V peroxo-tartrate complexes and their use as molecular precursors for Nb-Ta mixed oxides. *Inorganic Chemistry*, 44(5):1554-1562, 2005.
12. Bergbreiter, D. E. Using soluble polymers to recover catalysts and ligands. *Chemical Reviews*, 102(10):3345-3384, 2002.
13. Dickerson, T. J., Reed, N. N., and Janda, K. D. Soluble polymers as scaffolds for recoverable catalysts and reagents. *Chemical Reviews*, 102(10):3325-3344, 2002.
14. Skorobogaty, A. and Smith, T. D. Coordination and redox chemistry of some macromolecular systems. *Coordination Chemistry Reviews*, 53:55-226, 1984.
15. Schechter, B., Arnon, R., and Wilchek, M. Polymers in drug delivery: immunotargeting of carrier-supported cis-platinum complexes. *Reactive Polymers*, 25(2-3):167-175, 1995.
16. Jagur-Grodzinski, J. Biomedical application of functional polymers. *Reactive and Functional Polymers*, 39(2):99-138, 1999.
17. Avichezer, D., Schechter, B., and Arnon, R. Functional polymers in drug delivery: carrier-supported CDDP (cis-platin) complexes of polycarboxylates-effect on human ovarian carcinoma. *Reactive and Functional Polymers*, 36(1):59-69, 1998.
18. Ohya, Y., Masunaga, T., Baba, T., and Ouchi, T. Synthesis and cytotoxic activity of dextran-immobilizing platinum(II) complex through chelate-type coordination bond. *Journal of Macromolecular Science, Part A: Pure and Applied Chemistry*, 33(8):1005-1016, 1996.
19. Kalita, D., Sarmah, S., Das, S. P., Baishya, D., Patowary, A., Baruah, S., and Islam, N. S. Synthesis, characterization, reactivity and antibacterial activity of new peroxovanadium(V) complexes anchored to soluble polymers. *Reactive and Functional Polymers*, 68(4):876-890, 2008.
20. Boruah, J. J., Kalita, D., Das, S. P., Paul, S., and Islam, N. S. Polymer-anchored peroxo compounds of vanadium(V) and molybdenum(VI): Synthesis, stability, and their activities with alkaline phosphatase and catalase. *Inorganic Chemistry*, 50(17):8046-8062, 2011.
21. Islam, N. S. and Boruah, J. J. Macromolecular peroxo complexes of vanadium(V) and molybdenum(VI): Catalytic activities and biochemical relevance. *Journal of Chemical Sciences*, 127(5):777-795, 2015.

22. Boruah, J. J., Ahmed, K., Das, S., Gogoi, S. R., Saikia, G., Sharma, M., and Islam, N. S. Peroxomolybdate supported on water soluble polymers as efficient catalysts for green and selective sulfoxidation in aqueous medium. *Journal of Molecular Catalysis A: Chemical*, 425:21-30, 2016.
23. Das, S. P., Ankireddy, S. R., Boruah, J. J., and Islam, N. S. Synthesis and characterization of peroxotungsten(VI) complexes bound to water soluble macromolecules and their interaction with acid and alkaline phosphatases. *RSC Advances*, 2(18):7248-7261, 2012.
24. Khanna, V., Jain, M., Barthwal, M. K., Kalita, D., Boruah, J. J., Das, S. P., Islam, N. S., Ramasarma, T., and Dikshit, M. Vasomodulatory effect of novel peroxovanadate compounds on rat aorta: Role of rho kinase and nitric oxide/cGMP pathway. *Pharmacological Research*, 64(3):274-282, 2011.
25. Chatterjee, N., Anwar, T., Islam, N. S., Ramasarma, T., and Ramakrishna, G. Growth arrest of lung carcinoma cells (A549) by polyacrylate-anchored peroxovanadate by activating Rac1-NADPH oxidase signalling axis. *Molecular and Cellular Biochemistry*, 420(1-2):9-20, 2016.
26. Conte, V. and Floris, B. Vanadium and molybdenum peroxides: synthesis and catalytic activity in oxidation reactions. *Dalton Transactions*, 40(7):1419-1436, 2011.
27. Rivas, B. L., Pereira, E. D., Palencia, M., and Sánchez, J. Water-soluble functional polymers in conjunction with membranes to remove pollutant ions from aqueous solutions. *Progress in Polymer Science*, 36(2):294-322, 2011.
28. Calixto, G., Yoshii, A. C., Rocha e Silva, H., Stringhetti Ferreira Cury, B., and Chorilli, M. Polyacrylic acid polymers hydrogels intended to topical drug delivery: preparation and characterization. *Pharmaceutical Development and Technology*, 20(4):490-496, 2015.
29. Nurkeeva, Z. S., Khutoryanskiy, V. V., Mun, G. A., Sherbakova, M. V., Ivaschenko, A. T., and Aitkhozhina, N. A. Polycomplexes of poly(acrylic acid) with streptomycin sulfate and their antibacterial activity. *European Journal of Pharmaceutics and Biopharmaceutics*, 57(2):245-249, 2004.
30. Fonseca, M. J., Cabanes, A., Alsina, M. A., and Reig, F. Design of a new formulation for sustained release of gentamicin: a Carbopol hydrogel. *International Journal of Pharmaceutics*, 133(1-2):265-268, 1996.

31. Turos, E., Shim, J. Y., Wang, Y., Greenhalgh, K., Reddy, G. S. K., Dickey, S., and Lim, D. V. Antibiotic-conjugated polyacrylate nanoparticles: new opportunities for development of anti-MRSA agents. *Bioorganic & Medicinal Chemistry Letters*, 17(1):53-56, 2007.
32. Bhattarai, N., Gunn, J., and Zhang, M. Chitosan-based hydrogels for controlled, localized drug delivery. *Advanced Drug Delivery Reviews*, 62(1):83-99, 2010.
33. Xie, D., Yang, Y., Zhao, J., Park, J. G., and Zhang, J. T. A novel comonomer-free light-cured glass-ionomer cement for reduced cytotoxicity and enhanced mechanical strength. *Dental Materials*, 23(8):994-1003, 2007.
34. Rogers, F. B. and Li, S. C. Acute colonic necrosis associated with sodium polystyrene sulfonate (Kayexalate) enemas in a critically ill patient: case report and review of the literature. *Journal of Trauma and Acute Care Surgery*, 51(2):395-397, 2001.
35. Sood, M. M., Sood, A. R., and Richardson, R. Emergency management and commonly encountered outpatient scenarios in patients with hyperkalemia. In *Mayo Clinic Proceedings*, volume 82(12), pages 1553-1561, 2007, Elsevier.
36. Buysse, J. M., Huang, I. Z., and Pitt, B. PEARL-HF: prevention of hyperkalemia in patients with heart failure using a novel polymeric potassium binder, RLY5016. *Future Cardiology*, 8(1):17-28, 2012.
37. Guo, Y., Ying, Y., Mao, Y., Peng, X., and Chen, B. Polystyrene sulfonate threaded through a metal-organic framework membrane for fast and selective lithium-ion separation. *Angewandte Chemie*, 128(48):15344-15348, 2016.
38. Terao, K. Poly(acrylic acid) (PAA). *Encyclopedia of Polymeric Nanomaterials*, 1654-1658, 2015.
39. Abdelaal, M. Y., Makki, M. S., and Sobahi, T. R. Modification and characterization of polyacrylic acid for metal ion recovery. *American Journal of Polymer Science*, 2(4):73-78, 2012.
40. Karolewicz, B. A review of polymers as multifunctional excipients in drug dosage form technology. *Saudi Pharmaceutical Journal*, 24(5):525-536, 2016.
41. Passoni, L. C., Siddiqui, M. R. H., Steiner, A., and Kozhevnikov, I. V. Niobium peroxo compounds as catalysts for liquid-phase oxidation with hydrogen peroxide. *Journal of Molecular Catalysis A: Chemical*, 153(1):103-108, 2000.

42. Delley, B. From molecules to solids with the $DMol^3$ approach. *The Journal of Chemical Physics*, 113(18):7756-7764, 2000.
43. Delley, B. An all-electron numerical method for solving the local density functional for polyatomic molecules. *The Journal of Chemical Physics*, 92(1):508-517, 1990.
44. Vosko, S. H., Wilk, L., and Nusair, M. Accurate spin-dependent electron liquid correlation energies for local spin density calculations: a critical analysis. *Canadian Journal of Physics*, 58(8):1200-1211, 1980.
45. Zhou, J., Xiao, F., Wang, W. N., and Fan, K. N. Theoretical study of the interaction of nitric oxide with small neutral and charged silver clusters. *Journal of Molecular Structure: THEOCHEM*, 818(1):51-55, 2007.
46. Delley, B. A scattering theoretic approach to scalar relativistic corrections on bonding. *International Journal of Quantum Chemistry*, 69(3):423-433, 1998.
47. Bayot, D., Devillers, M., and Peeters, D. Vibrational spectra of eight-coordinate niobium and tantalum complexes with peroxo ligands: A theoretical simulation. *European Journal of Inorganic Chemistry*, 2005(20):4118-4123, 2005.
48. Nakamoto, K. *Infrared and Raman Spectra of Inorganic and Co-ordination Compounds, Part B.* Wiley and Sons, New York, 1997.
49. Rivas, B. L., Seguel, G. V., and Geckeler, K. E. Synthesis, characterization, and properties of polychelates of poly(styrene sulfonic acid-co-maleic acid) with Co(II), Cu(II), Ni(II), and Zn(II). *Journal of Applied Polymer Science*, 85(12):2546-2551, 2002.
50. Pourjavadi, A. and Ghasemzadeh, H. Carrageenan-g-poly(acrylamide)/ poly(vinylsulfonic acid, sodium salt) as a novel semi-IPN hydrogel: Synthesis, characterization, and swelling behavior. *Polymer Engineering & Science*, 47(9):1388-1395, 2007.
51. Silverstein, R. M., Bassler, G. C., and Morrill, T. C. *Spectrometric Identification of Organic Compounds,* John Wiley and Sons, Inc, Hoboken, New Jersey, 1991.
52. El Wahed, M. A., El Manakhly, K. A., and El Kososy, N. Physicochemical studies of hydroxyquinoline sulfonic acid and its transition metal complexes. *Materials Chemistry and Physics*, 41(2):117-122, 1995.
53. Cristovan, F. H., Nascimento, C. M., Bell, M. J. V., Laureto, E., Duarte, J. L., Dias, I. F., Cruz, W. O., and Marletta, A. Synthesis and optical characterization of

poly(styrene sulfonate) films doped with Nd(III). *Chemical Physics*, 326(2):514-520, 2006.

54. Feng, Y., Schmidt, A., and Weiss, R. A. Compatibilization of polymer blends by complexation. 1. Spectroscopic characterization of ion-amide interactions in ionomer/polyamide blends. *Macromolecules*, 29(11):3909-3917, 1996.
55. Jiang, D. D., Yao, Q., McKinney, M. A., and Wilkie, C. A. TGA/FTIR studies on the thermal degradation of some polymeric sulfonic and phosphonic acids and their sodium salts. *Polymer Degradation and Stability*, 63(3):423-434, 1999.
56. Maczka, M., Ptak, M., Majchrowski, A., and Hanuza, J. Raman and IR spectra of $K_4Nb_6O_{17}$ and $K_4Nb_6O_{17}\cdot 3H_2O$ single crystals. *Journal of Raman Spectroscopy*, 42(2):209-213, 2011.
57. McNeill, I. C. and Sadeghi, S. M. T. Thermal stability and degradation mechanisms of poly(acrylic acid) and its salts: Part 2–Sodium and potassium salts. *Polymer Degradation and Stability*, 30(2):213-230, 1990.
58. Jacobson, S. E., Tang, R., and Mares, F. Group 6 transition metal peroxo complexes stabilized by polydentate pyridinecarboxylate ligands. *Inorganic Chemistry*, 17(11):3055-3063, 1978.
59. Lapina, O. B., Khabibulin, D. F., Romanenko, K. V., Gan, Z., Zuev, M. G., Krasil'nikov, V. N., and Fedorov, V. E. ^{93}Nb NMR chemical shift scale for niobia systems. *Solid State Nuclear Magnetic Resonance*, 28(2):204-224, 2005.
60. Papulovskiy, E., Shubin, A. A., Terskikh, V. V., Pickard, C. J., and Lapina, O. B. Theoretical and experimental insights into applicability of solid-state ^{93}Nb NMR in catalysis. *Physical Chemistry Chemical Physics*, 15(14):5115-5131, 2013.
61. Flambard, A., Montagne, L., Delevoye, L., and Steuernagel, S. ^{93}Nb and ^{17}O NMR chemical shifts of niobiophosphate compounds. *Solid State Nuclear Magnetic Resonance*, 32(2):34-43, 2007.